行政院國家科學委員會專題研究計畫 成果報告

大白鼠 A7/A5 區域正腎上腺素神經元與三叉神經運動系統關係之研究(2/2)
研究成果報告(完整版)

計 畫 類 別 ：個別型
計 畫 編 號 ：NSC 94-2320-B-040-008-
執 行 期 間 ：94 年 08 月 01 日至 95 年 07 月 31 日
執 行 單 位 ：中山醫學大學生物醫學科學學系

計 畫 主 持 人：楊琇雯

計畫參與人員：1 共同主持人, 2-4 研究生：閔明源、吳玉威、施珮妤、林佳靜

處 理 方 式 ：本計畫涉及專利或其他智慧財產權，2 年後可公開查詢

中 華 民 國 95 年 11 月 09 日

Characteristics of noradreanergic (NAergic) and non-NAregic neurons in A7 catecholamine cell group: the role for type-A potassium currents.

Ming-Yuan Min[1, 2], Yu-Wei Wu[2, #], Pei-Yu Shih[2, #], Chia-Jin Lin[1], Hsiu-WenYang[3]

[1]Department of Life Science and [2]Institute of Zoology, National Taiwan University, Taipei 106, Taiwan
[3]Department of Biomedical Sciences, Chung Shan Medical University, Taichung 402, Taiwan

Correspondence should be addressed to:
Dr. Hsiu-Wen Yang
Department of Biomedical Sciences
Chung Shan Medical University
No. 110, Sec. 1, Chien-Kuo N. Road
Taichung 402, Taiwan

Running Title: I_A in NAergic Nreuons

Keywords: brainstem, Kv4, Nociception, Rats, Whole-cell recording

[#]The two authors contribute equally to this work

Abstract

The pontine noradrenergic (NAergic) neurons located in A7 area are believed to play an important role in modulating nociception. In this study we investigated their physiological and morphological properties. Sagittal brain stem slices were taken from rats aged 7-10 days; A7 neurons were identified by immunohistochemical staining for DBH, the synthesis enzyme of norepinephrine, after electrophysiological recording. Two types of neurons were encountered in A7 area: the large DBH-immunoreactive (ir) neurons and small non-DBH-ir neurons. In reflecting the difference in somata diameter, DBH-ir neurons, when compared to non DBH-ir neurons, have smaller input resistance and higher threshold for firing action potential. DBH-ir neurons also displayed some physiological properties, which were not seen in non DBH-ir neurons, i.e. the delayed onset of first spike and slow discharging rate upon injection of depolarizing current pulses. These differences were attributed to expression of large amount of Kv4.2 channel in DBH-ir neurons. Heterogeneity in firing patterns was observed among non DBH-ir neurons, suggesting there are different functional types of interneurons in A7 cell groups. These results provide first description of electrophysiological properties of noradrenergic and interneurons and possible interaction between these neurons in A7 area.

Introduction

Many morphological evidences have suggested that noradrenergic neurons in subcoeruleus nuclei, including the A7 and A5 catecholamine cell groups located, respectively, in lateral and ventral pontine area, might have anti-nociceptive effect by projecting their axons to the dorsal horn of spinal cord (Clark and Proudfit, 1991, 1993). In supporting of this, behavior studies have shown a significant anti-nociceptive effect in rats followed by a directly electrical or chemical stimulation of A7 catecholamine cell group (Yeomans and Proudfit, 1992), as well as by intrathecal injection of norepinephrine (NE) with NE acting at α1 and α2-adrenoreceptors (Howe et al., 1983; Loomis and Arunachalam, 1992; Reedy et al., 1980; Yeomans, and Proudfit, 1992**)**. Moreover, it has also been shown that the well known antinociceptic effect induced by electrical stimulation of neurons in per-aqucdal gray area (PGA) (Barbaro et al., 1985; Basbaum et al., 1984) is reduced following lesion made to A7 catecholamine cell group, suggesting PAG may exert some of it's antinociceptic effect uvia modulating A7 catecholamine cell group (Bajic and Proudfit, 1999; Clark and Proudfit 1991; Holden et al, 1999; Nuseir and Proudfit, 2000; Proudfit and Monsen, M. 1999). Nevertheless, detailed mechanism underlying the anti-nociceptic effect of A7 catecholamine cell group at cellular level is still a mater of some debts as there is, in literature, no reports that has systemically worked on the intrinsic physiological property of neurons in A7 catecholamine cell group. This might be partially due to the very small neuronal number in the A7 area, which make it difficult to identify catecholamine cells in A7 area for electrophysiological recording both in vivo and in vitro.

The fast activated and inactivated A-type potassium current (I_A) is believed to play important roles in governing the spike shape, firing frequency, and synaptic integration and plasticity in many neurons (Rudy et al., 1999; Johnston et al., 2000; Ishikawa et al, 2003). Recently, it has been reported that large I_A mediated by Kv 4.2 channel can be evoked in neurons located in lamina I of dorsal spinal cord, which are involved in conveying nociceptic signal in the central nervous system. Moreover, it has been shown that kinase system, such as PKA, PKC and MAP kinase, activated during central sensitization can down regulated I_A , which in turn increases excitability of dorsal horn neurons and provide possible mechanism for central sensitization (Adams et al., 2000; Anderson et al., 2000; Hu et al., 2003; Hu et al., 2006). In this study, we set out to make whole cell recording form noradrenergic (NAergic) neurons in vitro, and explore a role for I_A in physiological property of NAergic neurons in A7 area. Preliminary results have been reported in abstract form (Min et al, 2004; Yang et al., 2004).

Material and Methods

Preparation of brain stem slices

The use of animals in this study was in accordance with the rules of the local ethical committee for animal research of National Taiwan University. The preparation of saggital brain stem slice has been described in a previous work (Min and Appenteng, 1996; Min et al., 2003). Briefly, wistar rats aged 7-10 days were decapitated. The brain was exposed, chilled with ice-cold artificial cerebrospinal fluid (ACSF), and saggital brainstem slices of 300 μm thickness, comprising the Vmot and surrounding regions, were cut with a vibroslicer (Campden, Loughborough, England). The ACSF contained (in mM): NaCl 105, KCl 5, $MgSO_4$ 1.3, $NaHCO_3$ 24, NaH_2PO_4 1.2, $CaCl_2$ 2, and glucose 10; pH adjusted to 7.4 by gassing with 95% O_2 /5% CO_2. The slices were kept in an interface-type chamber at room temperature (24-25°C) to allow recovery for at least 90 minutes.

Visualization of trigeminal interneurones and whole cell patch clamp recording

Slices were transferred to an immersion-type recording chamber mounted to an upright microscope (BX51WI, Olympus Optical Co., Ltd., Tokyo, Japan), equipped with water-immersion objectives, a Normaski optic system, an infrared filter and a CCD camera. Neurones located ~ 200 μm rostral to the anterior border of Vmot were recorded with patch pipettes using procedures described by Stuart *et al*. (1993). Patch pipettes were pulled from borosilicate glass tubing (1.5 mm outer diameter, 0.5 mm wall thickness; Warner Instruments Corp., Hamden, CT, USA), and had a resistance of 5-8 MΩ when filled with internal solution. The internal solution contained (in mM): potassium gluconate 100, EGTA 10, $MgCl_2$ 5, Hepes 40, ATP 3; GTP 0.3; pH adjusted to 7.2 by

KOH and osmolarity to 295 mOsm by sucrose. Once the whole cell recordings were obtained, the patch amplifier (Multiclamp 700B; Axon Instruments Inc.; Union City, CA, USA) was set to either current- or voltage-clamp mode to character the basic firing pattern and I_A, respectively. For current clamp recording, the bridge was balanced by adjusting the serial resistance compensation of the amplifier. Neurones were only accepted for further study if the membrane potential (Vm) was at least -45 mV without applying holding current, and the spike overshot 0 mV. Signals were low-pass filtered at a corner frequency of 2kHz and then digitized at 10 kHz using a Micro 1401 interface running Signal software provided by CED (Cambridge Electronic Design, Cambridge, UK).

For voltage-clamp recording, 1μM Tetrodotoxin (Tocris) was routinely added in, while calcium was omitted from, aCSF to isolate potassium current. After breaking through plasma membrane, the serial resistance was < 15 MΩ and was compensated by at least 75%. The estimated junction potential was ~ 2mV and was not corrected. Signals were low-pass filtered at a corner frequency of 2kHz and then digitized at 10 kHz using a Micro 1401 interface running Signal software provided by CED (Cambridge Electronic Design, Cambridge, UK). Leak subtraction was made off-line in Signal software. The membrane voltage was held at -70 mV, and I_A were isolated by a two-step protocol as described in the result. To determine the voltage-dependent activation, voltage steps of 1 s were applied at 3 s intervals in 10 mV increments from -90 mV to a maximum of +10 mV. To determine the voltage-dependent inactivation, conditioning pre-pulses ranging from -90 mV to -20 mV were applied at 3 s intervals in +10 mV increments for 1 s

followed by a step to 0 mV for 800 ms. To determine time-dependent recovery from inactivation, conditioning pulses (from -100 mV to +10 mV) were applied for 800 ms in 10 ms incremental duration from 10 ms to 200 ms.

Filling recorded interneurones with biocytin and histology

In all of the experiments, 10 mM biocytin (Sigma, St. Louis, MO, USA) was routinely included in the internal solution to fill the recorded neurones. Neurones were filled by passive diffusion of biocytin from the patch pipette during the recording period, without application of current. After recording, pipettes were withdrawn and slices left in the recording chamber for additional 30 minutes to allow for biocytin transport within the dendrites and axon. The brain slices were then fixed overnight in 4% paraformaldehyde (Sigma) in 0.1 M phosphate buffer (PB, pH 7.4) at 4° C. Slices were rinsed with PB several times after fixation and were subject to immunostaining procedures without further sectioning. Briefly, slices were rinsed in 0.03% Triton X-100 in phosphate-buffered saline (TPBS), and incubated for 1 hr at room temperature in TPBS containing 2% bovine serum albumin (BSA), 10% normal goat serum (NGS), and 10% normal horse serum (NHS). The slices were then incubated overnight at 4°C in TPBS containing a 1/1500 dilution of mouse antibody against DBH (Chemicon, Temecula, CA, USA) and a 1/200 dilution of avidin-AMCA (Vector Laboratories, Burlingame, CA, USA). After rinses in TPBS, the slices were incubated with fluorescein isothiocyanate (FITC)-conjugated goat anti-mouse IgG antibodies (Jackson, Pennsylvania, USA) diluted 1/50 in TPBS. The slices were then observed under a fluorescent microscopy (Olympus BX50, Tokyo, Japan). In some experiments, slices were first incubated with cocktail containing

antibody against DBH, avidin-AMCA, avidin-biotinylated Horseradish peroxidase complex (ABC kit, 1/200 dilution, Vector Laboratories, Burlingame, CA, USA). They were then reacted with FITC- conjugated goat anti-mouse IgG antibodies, and observed under fluorescent microscopy for identification of cell type. After fluorescent microscopic observation, slices were treated with 3% H_2O_2 in 0.1 M PB for 20 min, and finally visualized again with 3,3'-diaminobenzidine (DAB) as a chromogen. The resulted staining of biocytin-filled neurones were examined, photographed, and reconstructed with an Olympus BX-50 microscope and a camera lucida drawing tube (SZX-DA, Olympus Optical Co., Ltd., Tokyo, Japan). The drawings of the reconstructed biocytin-filled neurones were digitised using a PC based scanner, and measurements made of soma minimum diameter, soma maximum diameter, dendrite segment length and branching of the axonal collaterals, using NIH-Image software (downloaded from the National Institute of Health website http://www.nih.gov). The soma surface area was determined by assuming an elliptical soma shape, and then calculated as: (major diameter/2) ×(minor diameter/2) ×π. All data given are expressed as mean ± standard error, and unless specified, a Mann-Whitney *U*-test was used for statistical comparison.

Single-Cell RT-PCR analysis

Protocols for single-cell RT–PCR experiments were modified from Liss et al. (1999). The patch pipettes were filled with ~10 µl of autoclaved internal solution containing: 140 mM KCl, 5 mM HEPES, 5 mM EGTA, 3 mM MgCl2, pH 7.3. At the end of the recording (~1 min), the cell contents were aspirated as completely as possible into the patch pipette under visual control by application of gentle negative pressure. Cells were only analysed

further when the whole-cell configuration remained stable throughout the harvesting proceedure. Pipettes were then quickly removed from the cell, washed twice through the solution interface, and the pipette contents were expelled immediately into a 0.5 ml test tube containing the lysis buffer with β-ME to block RNase activity. RNA was purified by Absolutrly RNA Nanoprep Kit (Stratagene, US) which includes treatment of DNase I for digestion of genomic DNA. First strand cDNA was then synthesized for 1 h at 50°C in a total reaction volume of 20 μl containing oligo$(dT)_{15-20}$ primers (Invitrogen, US; final concentration 25 ng/μl), dithiothreitol (final concentration 10 mM), the four deoxyribonucleotide triphosphates (Invitrogen, final concentration 0.5 mM each), 20 U of ribonuclease inhibitor (Invitrogen) and 100 U of reverse transcriptase (Superscript™III; Invitrogen). The single-cell cDNA was kept at –20°C until PCR amplification.

Following reverse transcription, the cDNAs for Kv1.4, Kv3.4, Kv4.2, Kv4.3 and DBH were amplified simultaneously in a multiplex PCR using the following sets of primer: Kv1.4-F3 : 5'-CTCAAGGAAGCCGAGGTAGT-3'(GenBank accession number NM_012971, pos. 307) Kv1.4-R3 : 5'-CGTTCACAACAGTCACTGTA-3'(613); Kv3.4-F1 : 5'- GAGGAGACCAGTTGCAATAC - 3' (GenBank accession number NM_145922, pos. 2737), Kv3.4-R1: 5'-CTTTATTGGTACTCGAGCAC-3' (2985); Kv4.2-F2: 5'-GCTCTGCCCACCATGACTGC-3'(GenBank accession number NM_031730.2, pos. 1034), Kv4.2-R1: 5'-AATAGGGTAGGATGGCCACC-3'(1373); Kv4.3-F1: 5'-TCAGCTTCCGCCAGACCATG-3'(GenBank accession number NM_031739, pos. 546), Kv4.3-R1: 5'-AATAGGGCATGATGGCCACC-3'(850); and DBH-F2: 5'-CACCACATCATCATGTATGAGGCC-3' (GenBank accession number

NM_013158, pos. 745), DBH-R2: 5'-CCTGGCGAGCACAGTAATCACC-3'(1293). First multiplex-PCR was performed as hot start in a final volume of 20 µl containing the 20 µl reverse transcription reaction, 100 nM of each primer, 0.2 mM each dNTP , 1.5 mM $MgCl_2$, 50mM KCl, 20 mM Tris–HCl (pH 8.4) and 1 U of *Taq* polymerase (Invitrogen) in a Peltier Thermal Cycler TC-200 with the following cycling protocol: after 3 min at 94°C, 35 cycles (94°C, 30 s; 60°C, 30 s; 72°C, 1 min) of PCR were performed followed by a final elongation period of 7 min at 72°C.

The nested-PCR amplifications were carried out in five individual reactions, in each case with 1 µl of the first PCR product under same PCR conditions using the following primer pairs: Kv1.4-F1: 5'-AGAAGATCCTTAGGGAGCTG-3'(424) Kv1.4-R1: 5'-ACTGTA GCGGACTGAACTGT-3'(599); Kv3.4-F1: 5'-GAAGATGCGTCAATAGCAG- 3' (2779), Kv3.4-R1: 5'-CTAGGCGTGCCTCAGACACA-3' (2920); Kv4.2-F2: 5'-CCGT CTCAGTCATCGATCGCGAAT-3'(1140), Kv4.2-R1: 5'-TACTCATGACACYGCGCA CA-3'(1343); Kv4.3-F1: 5'-CGGTGCCATGCGGCACGGTG-3'(669), Kv4.3-R1: 5'-AT GCTCATCACACTGCGGAT-3'(840); and DBH-F3: 5'-TCAACTACTGTCGCCACGT GC-3' (890), DBH-R3: 5'-ACCAGTCCAAGCTCCATGATGC-3'(1124).

To investigate the presence and size of the amplified fragments, 10 µl of the PCR products were separated and visualized in an ethidium bromide-stained agarose gel (2%) by electrophoresis. The predicted sizes (bp) of the five PCR-generated fragments were: 176 (Kv1.4), 142 (Kv3.4), 204 (Kv4.2), 172 (Kv4.3) and 235 (DBH).

Results

In longitudinal brainstem sections, cut from brain of animals receiving intramuscular injection of 1% true blue made in masseter muscle and subsequently subject to immunostaining using antibodies against TH and DBH, two populations of neurons showing both TH-ir and DBH-ir could be identified in the rostral and ventral border of trigeminal motor nucleus (Fig.1A-C). These results indicate that these two groups of neuron are mostly noradrenergic but not dopaminergic, and are presumed to be the A7 and A5 cell groups, respectively (Min et al, 2006; Paxinos and Watson, 1998). In the fresh brainstem slices of the presume A7 area (i.e. ~200 μM rostral to Vmot; cf. Fig. A and D), two types of neurons could easily identified according to the diameter of their soma using IR-DIC optics (Fig.1D, E, F). We first made whole-cell recording and injected biocytin to the both types of neurons without any selection, and a total number of 81 neurons were recorded. The recorded neurons are classified into three categories basing on the results of immunostaining using antibody against DBH made following electrophysiological recording. The first group of recorded and biocytin labeled neurons were those found non DBH-ir and located outside A7 area, defined as where DBH-ir neurons aggregates (Fig. 1I); this group of neurons accounts for 38 % (31/81) of total recorded neurons and are discarded without further analysis. The second group of neurons were also non DBH-ir, but were located within DBH-ir neurons (Fig. 1J-L), i.e. in the A7 area; this group of neurons accounts for 27% (22/81) of total recorded neurons. The third group of neurons is DBH-ir neurons (Fig. 1G&H); they accounts for 35% (26/81) of total recorded neurons.

Measurements are made of membrane and spike properties from the second and third groups of recorded neuron (Fig. 2A, B, C), and are summarized in Table 1. No significant difference is found between the two groups of neurons in most of parameters examined, except for input resistance, rheobase (defined as minimum intensity of depolarizing current pulse required for firing), and membrane time constant. The DBH-ir neurons have significantly smaller input resistance, higher rheobase, and shorter membrane time constant than that of non–DBH ir neurons Table 1. These results indicate that DBH-ir neurons may have much larger somatic diameter than the non DBH-ir neurons have (see Fig. 1E-H, J-L). This possibility is confirmed by morphological measurement, which shows that the averaged somatic diameter of DBH-ir neurons is ~ 1.7 folds larger than that of non DBH-ir neurons (22 ± 0.7 μm *vs.* 13 ± 2.1 μm ; $p < 0.01$, *Mann-Whitney U-test*). In addition, in response to the injection of depolarizing current ramp, the maximum firing rate of DBH-ir neurons is slower than the non DH-ir neurons (Fig. 2D, E; Table 1).

The non DBH-ir neurons show great diversity in the spiking pattern; at least they can be further grouped into three categories according to firing pattern. The first group of non DBH-ir neurons fired repeatedly and regularly, and showed moderate delay in firing first action potential upon depolarizing current injection (Fig. 3A). This type of non-DBH-ir neurons could be further divided into two subgroups, with one typed neurons showing rebound action potential following recovery from injection of hyperpolarizing current pulse, while the other type do not show this property (Fig. 3B). For the last type of non DBH-ir neuron, significant spike adaptation is seen upon injection of depolarizing current

pulse (Fig. 3C). In contrast to the non DBH-ir neurons, the firing pattern of DBH-ir neurons is very homogenous. A very impressed feature seen in almost all DBH-ir neurons recorded in this study is that the neurons showed very prominent delay in firing the first action potential upon injection of depolarizing current pulse, and once excited, they fire train of spikes very regularly with lowly (Fig.3 D). This feature is more clearly seen when the response of membrane voltage to a depolarizing current ramp injected into the cells is examined. As shown in Figure 3E, the relationship between the increasing intensity of current ramp and the increasing membrane voltage was linear, and before the onset of action potential, membrane voltage however showed rectification in direction of repolarization (Fig. 3 E). When steady state depolarizing current was injected into neurons to make them constantly fire, delay in action potential initiation can be also seen after termination of hyperpolarization induced by applying a further hyperpolarizing current pulse (Fig. 3D).

The fast activated and inactivated A-type potassium current (I_A) may provide best candidate ionic mechanism underlying delay onset of action potential found in DBH-ir neurons in A7 area. To test this possibility, we examined if I_A could be elicited in these neurons. As shown in Fig. 4A, voltage step from –100 to 0 mV evoked a transient outward current that decay quickly and leveled off at about 39.67% of peak amplitude with time constant of 48.88 ms. Voltage step from –30 to 0 mV however evoked slowly activated but sustained outward current with peak current amplitude equaling to the leveled off part of current evoked from –100 mV (Fig. 4B). Subtracting current evoked from –30 mV from that evoked from –100 mV yield component that, in response to

voltage step, is quickly activated and completely decayed (Fig. 4C). In addition, this subtracted current was blocked by 4-AP, a non selective I_A blocker, with IC_{50} at 1.5 mM (Fig. 4D). These results show that large I_A can be constantly evoked by almost all DBH-ir neurons tested. In contrast to DBH-ir neurons, peak amplitude of I_A evoked in non DBH-ir neurons was not as large as in the DBH-ir neurons (fig. 5A). Because the non DBH-ir neurons is substantially smaller than the DBH-ir neurons, for comparison, we normalize the total amount of charge transferred underlying evoked I_A by the somatic surface to obtain charge density I_A of the recorded neurons, and found that value obtained from DBH-ir neurons is much higher than that obtained from that of non-DBH-ir neurons (Fig. 5B). These results suggest that prominently delay in the onset of first action potential observed in DBH-ir neurons but not in non DBH-ir neurons might be abscribed to activation of I_A.

We next examined the gating kinetic of I_A evoked in DBH-ir neurons, including the steady state activation and inactivation, and recovery from inactivation. As shown in Fig. 6A, activation of I_A starts at –60 ~ -50 mV with half activated at about –30 mV. For inactivation and recovery, the I_A is approximately half inactivated at Vm about –70 mV (Fig. 6B), and it recovers from inactivation very quickly with recovering time constant being 21.87 ms (Fig. 6C). The above results indicate that I_A evoked in DBH-ir neurons has gating properties of low threshold for activation, and inactivated and recovery from inactivated very quickly; these gating features favor that the evoked I_A is mediated by Kv4 subfamily of voltage-dependent potassium channels. We tested this possibility by examining the effect of 500nM heteropodatoxin (HpTx) venom toxin that selectively

blocks Kv4 channel (Sanguinetti et al., 1997), on I_A evoked in DBH-ir neurons. As shown in Fig. 7A, I_A is attenuated by HpTx by 38.64 % (n = 4 cells tested; $p<0.01$ paired t test), showing that Kv4 channels are involved in mediating I_A in DBH-ir neurons. We also checked the effect of 1 μM BDS-1, a selective blocker of Kv3.4 (Diochot et al., 1998), on I_A in DBH-ir neurons. As shown in Fig. 7B, application of BDS-1 has no significant effect on I_A (96.7 % of control; n = 3; $p > 0.2$, paired t test), indicating no role for Kv3.4 channel in mediating I_A in DBH-ir neurons.

In order to prove that I_A directly contributes to the prominent delay in firing action potential in DBH-ir neurons, we went on to examine the impact of blocking I_A on spiking pattern in DBH-ir neurons. Because channel mediating I_A in DBH-ir neurons is almost completely inactivated at Vm about –40 mV, we first test whether delay in initiation of action potential is voltage-dependent. As shown in Fig. 8A, delay in the initiation of action potential in response to depolarizing current injected using TTL was not seen, when the membrane potential was depolarized to about –45 mV. Similarly, in the present of 10 mM 4-AP or 500 nM HpTx delay in initiation of action potential was also blocked in 4 cells tested for 4-AP and 3 cells for HpTx, even when the membrane potential was hold at –80 ~ -90 mV (Fig. 8B and 8C). Delay of firing after termination of hyperpolarizing current injection was also blocked by bath application of 4-AP in neurons which was excited to continuously fire. These results therefore support the argument that Kv4 channels mediated fast activated and inactivated I_A can result in the prominently delay in onset of action potential in DBH-ir neurons in A7 area.

Finally, to further identify the molecular composition of channels contribute to the I_A in DBH-ir neurons, we combined patch-clamp recording and single-cell RT-PCR technique to probe for the expression of the candidate genes of Kv1.4, Kv3.4, Kv4.2 and Kv4.3. Specific primer pairs for Kv1.4, Kv3.4, Kv4.2, Kv4.3 and DBH were designed to amplify cDNA products reverstranscript from mRNA of single neuron. cDNA products obtained from total brainstem tissue were used as templates in positive control experiments to confirm the specificity of each primer pairs (Fig. 9B), while cDNA products obtained from internal solution of patch-pipette without extracting cell content were used as templates in negative control experiments to rule out the tissue contamination (Fig. 9C). The results showed that gene of Kv4.2 but not Kv4.3 expressed in DBH expressing neurons (Fig. 9A), suggesting that I_A evoked in NAergic neurons of A7 catecholamine cell group was mediated by Kv4.2 channel.

Discussion

In this study we provide first description of electrophysiological and morphological properties of noradrenergic neurons in A7 catecholamine cell group. The most impressed feature for these neurons is that, in response to depolarizing current injection, initiation of action potential is difficult, with prominent delay before the discharging action potential clearly seen. This property is attributed to the expression of large amount of Kv4 subfamily of voltage- dependent potassium channels that mediate I_A in noradrenergic neurons in A7 area. In addition, presumed local interneurons, displaying different physiological properties, are also found in the A7 area. The morphological observation indicates that there are synaptic connections between these presumed interneruons with the noradrenergic neurons.

Currently, among the superfamily of voltage-dependent potassium channel, the putative α subunits meditating I_A include Kv 1.4, Kv 3.4, kv4.2, and Kv 4.3 (Jerng et al., 2004). In NAergic neurons of A7 catecholamine cell group, the evoked I_A had properties of fast activation at low threshold (~ -70 mV), fast inactivation with the time constant of 60.62 ± 3.10 ms and half inactivation point at -70 mV, and quickly recovering from inactivation with time constant of 21.87 ± 2.80 ms. According to the previous studies on cloned Kv channels expressed in oocytes or other cell lines (Coetzee et al., 1999), all of the gating properties indicate that I_A evoked here might be mediated by Kv4 channels. This argument is further supported by the flowing pharmacological results. First, as it has been reported that I_A mediated by Kv1.4 channel is more sensitive to 4-AP than Kv4 channels are, with IC_{50} of Kv1.4 channel being ~ 2 folds less than that of Kv4 channel (~0.7 vs

~1.5 mM; Yao and Tseng, 1994; Song et al., 1998; Tseng, 1999); our result showing that I_A evoked in NAergic neurons could only be attenuated by high concentration of 4-AP with IC_{50} of ~ 1.5 mM, would favor for Kv4 channels mediating current. Second, our results also show that I_A evoked in NAergic neurons was unaffected by BDS-1, a specific Kv3.4 channel blocker (Diochot et al., 1998), therefore ruling out the involvement of Kv3.4. Finally, the evoked I_A was attenuated by specific Kv4 channels, HpTx2, confirming a Kv4 mediated current (Sanguinetti et al., 1997). Moreover, single-cell RT-PCR analysis showed constant expression of Kv4.2 but not Kv4.3 channel in DBH expressing neurons, suggesting that I_A evoked in NAergic neurons of A7 catecholamine cell group was mediated by Kv4.2 channel. The Kv4 subfamily of voltage-dependent potassium channels has been reported to play important role in governing many functions of neuron, such as the neuronal excitability, firing pattern, synaptic integration and plasticity (Rudy et al., 1999; Johnston et al., 2000; Ishikawa et al, 2003). In NAergic neurons of A7 catecholamine cell group, upon the blockage I_A of by 4-AP and HpTx, a significantly increasing in spike half width and firing frequency indicates that I_A is involved in action potential repolarization and discharging frequency in this neuron. Moreover, dramatic reduction in delay of spike initiation suggests I_A also plays important role in synaptic integration. The threshold for initiation action potential in NAergic neurons is about -40 mV (Table 1), which is lower than that for I_A activation. It is therefore very easily for the fast, transiently synaptic input to be shunted down by I_A before the Vm to be depolarized to action potential threshold by the synaptic input. In such a circumstance, in order to drive NAergic neurons to fire action potential, the presynaptic neurons have to continuously discharge, so that depolarization caused by

temporally summarized synaptic input can be sustained long enough to inactive I_A, and drive NAergic neurons to fire. In view of the important role of NAergic neurons in modulating nociceptive afferent by releasing NE in dorsal horn of spinal cord as suggested by many previous studies (Holden and Pizzi, 2003), it is theoretically possible that downregulation of I_A would enhance excitability of NAergic neurons and efficacy of integration of excitatory input on to them, and therefore enhance their antinociceptive effect. In fact, similar mechanism has been proposed for the nociceptive afferent pathway; it has been reported that activation of PKA, PKC, MAP/ERK kinase can downregulate I_A in cultured dorsal horn neurons, which might be underlying central sensitization of nociception (Hu and Gereau, 2003; Hu et al., 2006).

In conclusion, we have successfully and specifically recorded neurons that are either immunopositive or negative to DBH, and are presumed to be, respectively, NAergic and non-NAregic neurons in the A7 catechalomine cell group. We have also explored a role for Kv4.2 channels mediated I_A in modulating repolarization of action potential, firing frequency and synaptic integration in NAergic neurons. These results will provide us a better insight to how A7 catecholamine cell group is involved in descending antinociceptive pathways.

References

Adams, J.P., Anderson, A.E., Varga, A.W., Dineley, K.T., Cook, R.G., Pfaffinger, P.J., Sweatt, J.D. (2000). The A-type potassium channel Kv4.2 is a substrate for the mitogen-activated protein kinase ERK. *J Neurochem.* **75,** 2277-2287.

Anderson, A.E., Adams, J.P., Qian Y., Cook, R.G., Pfaffinger P.J., Sweatt J.D. (2000). Kv4.2 phosphorylation by cyclic AMP-dependent protein kinase. *J Biol Chem.* **275,** 5337-5346

Bajic, D., and Proudfit, H.K. (1999). Projections of neurons in the periaqueductal gray to pontine andmedullary catecholamine cell groups involved in the modulation of nociception. *J. Comp. Neurol* **405,** 359-379.

Bajic, D., Proudfit H.K., Van Boskstaele, E.J. (2000) Periaqueductal gray neurons monosynaptically innervate extranuclear noradrenergic dendrites in the rat perirol. *J Comp. Neurol.* **427**, 649-662.

Barbaro, N.M., Hammond, D.L., and Fields, H.L. (1985). Effects of intrethecally administered methysergide and yohimbide on microstimulation-produced antinociception in rats. *Brain Res.* **343,** 233-229.

Basbaum, A.I., and Fields, H.L. (1984). Endogenous pain control system: brainstem spinal pathways and endorphin circuits. *Annu. Rev. Neurosci.* **7,** 233-255.

Clark, F.M., and Proudfit, H.K. (1991). The projection of noradrenergic neurons in the A7 catecholamine cell group to the spinal cord in the rat demonstrated by anterograde tracing combined with immunocytochemistry. *Brain Res.* **547,** 279-288.

Clark, F.M., and Proudfit, H.K. (1993). The projection of noradrenergic neurons in the A5catecholamine cell group to the spinal cord in the rat: Anatomical evidences that A5 neuronsmodulate nociception. *Brain Res.* **616,** 200-210.

Coetzee, W.A., Amarillo, Y., Chiu, J., Chow, A., Lau, D., McCormack, T., Moreno, H., Nadal, M.S., Ozaita, A., Pountney, D., Saganich, M., Vega-Saenz de Miera, E., Rudy B. (1999). Molecular diversity of K^+ channels. *Ann N Y Acad Sci.* **868,** 233-285.

Diochot, S., Schweitz, H., Beress, L., Lazdunski, M. (1998). Sea anemone peptides with a specific blocking activity against the fast inactivating potassium channel Kv3.4. *J Biol Chem.* **273,** 6744-6749.

Grzanna, R., Chee, W.K, and Akeyson, E.W. 1987. Noradrenergic projections to brainstem nuclei: evidence for differential projections from noradrenergic subgroups. *J Comp Neurol.* **263,** 76-91.

Holden, J.E., Pizzi, J.A. (2003) The Challenge of chronic pain. *Adv. Drug Deliv. Rev*. **55**, 935-948.

Holden, J.E., Schwartz, E.J., and Proudfit, H.J. (1999). Microinjection of morphine in the A7 catecholamine cell group produces opposing effect of the nociception that are mediated by adrenoceptors. *Neurosci.* **91,** 979-990.

Howe, J.R., Wang, J.-Y., and Yaksh, T.L. (1983). Selective antagonism of the antinociceptive effectof intrathecally applied-agonist by intrathecal prazosin and intrathecal yohimbine. *J. Pharmac.Exp. Ther.* **224,** 552-558.

Hu, H.J., Carassquillo, Y., Karim, F., Jung, W.E., Nerbonne, J.M., Schwarz, T.L., Gereau, R.W. (2006) The kv4.2 potassium channel subunits is required for pain plasticity. *Neuron* **50**, 89-100.

Hu, H.J., Glauner, K.S., Gereau, R.W. 4th. (2003). ERK integrates PKA and PKC signaling in superficial dorsal horn neurons. I. Modulation of A-type K^+ currents. *J Neurophysiol.* **90,** 1671-1679.

Ishikawa ,T., Nakamura Y., Saitoh, N., Li W.B., Iwasaki S., Takahashi T. (2003). Distinct roles of Kv1 and Kv3 potassium channels at the calyx of Held presynaptic terminal. *J Neurosci.* **23,** 10445-10453.

Jerng, H.H., Pfaffinger, P.J., Covarrubias, M. (2004). Molecular physiology and modulation of somatodendritic A-type potassium channels. *Mol Cell Neurosci*. **27,** 343-369.

Liss, B., Bruns, R., Roeper, J.(1999). Alternative sulfonylurea receptor expression defines metabolic sensitivity of K-ATP channels in dopaminergic midbrain neurons. *EMBO J.* **18,** 833-46.

Loomis, C.W., Arunachalam, K.D. (1992). Intrathecal St-587: effect on nociceptive reflex and bloodpressure in the rat. *J. Pharmac. Exp. Ther.* **263,** 482-453.

Lyons, W.E., Grzanna, R. (1988). Noradrenergic neurons with divergent projections to the motor trigeminal nucleus and the spinal cord: a double retrograde neuronal labeling study. *Neuroscience* **26,** 681-693.

Min, M.-Y., Appenteng, K. (1996) Multimodal distribution of amplitudes of miniature and spontaneous EPSPs recorded in rat trigeminal motoneurones. *J. Physiol.* **494**, 171-182.

Min, M.-Y., Hsu, P.-C., and Yang, H.-W. (2003). The physiological and morphological characteristics of interneurons caudal to the trigeminal motor nucleus in rats. *Eur. J. Neurosci.* **18,** 2981-2998.

Min, M.Y., Hsu, P.C., and Yang HW (2004) Whole cell recording from neurons located in pontine A7 nucleus in rat brainstem slices. Program No. 521.10. 2004 Abstract Viewer/Itinerary Planner, Washington, DC: Society for Neuroscience, 2004. Online：http://sfn.scholarone.com/.

Min, M.-Y., Hsu, P.-C., Lu, H.-W., Lin1, C.-J., Yang, H.-W. (2006) Postnatal development of noradrenergic terminals in the rat trigeminal motor nucleus: a light and electron microscopic immunocytochemical analysis. *Ana. Rec*. (in press).

Nuseir, K., and Proudfit, H.K. (2000). Bidirectional modulation of nociception by GABA neuronsin the dorsolateral pontine tegmentum that tonically inhibt spinall projecting noradrenergic A7 neurons. *Neurosci.* **96,** 773-783.

Paxinos, G., Watson, G. (1998). The Rat Brain in Stereotaxic Corodinates. San Diego: Academic Press.

Proudfit, H.K., and Monsen, M. (1999). Ultrastructure evidence that substance P neurons form synapses with noradrenergic neurons in the A7 catecholamine cell group that modulate nociception.*Neurosci.* **91,** 1499-1513.

Reedy, S.V.R., Maderdrut, J.L., and Yaksh, T.L. (1980). Spinal cord pharmacology of adrenergic agonist-mediated antinociception. *J. Pharmac. Exp Ther.* **213,** 525-553.

Sanguinetti, M.C., Johnson, J.H., Hammerland, L.G., Kelbaugh P.R., Volkmann R.A., Saccomano N.A., Mueller A.L. (1997) Heteropodatoxins: peptides isolated from spider venom that block Kv4.2 potassium channels. *Mol Pharmacol.* **51,** 491-498.

Satoh, M., Oku, R., and Akaike, A. (1993). Analgesia produced by microinjection of L-glutamate into rostral ventromedial bulbar nuclei of the rats and its inhibition by intrathecal adrenergic blocking agents. *Brain Res.* **261,** 361-364.

Schrader, L.A., Anderson, A.E., Mayne, A., Pfaffinger, P.J., Sweatt, J.D.(2002).PKA modulation of Kv4.2-encoded A-type potassium channels requires formation of a supramolecular complex. *J Neurosci.* **22(23),** 10123-33.

Song, W.J., Tkatch, T., Baranauskas, G., Ichinohe, N., Kitai S.T., Surmeier, D.J. (1998). Somatodendritic depolarization-activated potassium currents in rat neostriatal cholinergic interneurons are predominantly of the A type and attributable to coexpression of Kv4.2 and Kv4.1 subunits. *J Neurosci.* **18,** 3124-3137.

Tseng, G.N. (1999). Different state dependencies of 4-aminopyridine binding to rKv1.4 and rKv4.2: role of the cytoplasmic halves of the fifth and sixth transmembrane segments. *J Pharmacol Exp Ther.* **290,** 569-577.

Vornov, J.J., Sutin, J. (1983). Brainstem projections to the normal and noradrenergically hyperinnervated trigeminal motor nucleus. *J Comp Neurol* **214,** 198-208.

Vornov, J.J., Sutin, J. (1986). Noradrenergic hyperinnervation of the motor trigeminal nucleus: alternations in membrane properties and responses to synaptic input. *J Nuerosci* **6,** 30-37.

Yao, J.A., Tseng, G.N. (1994). Modulation of 4-AP block of a mammalian A-type K channel clone by channel gating and membrane voltage. *Biophys J.* **67,** 130-142.

Yang, H.W., and Min, M.Y. (2004). The excitatory and inhibitory synaptic activity recorded from adrenergic neurons of a7 area in rats. Program No. 521.9. 2004 Abstract Viewer/Itinerary Planner.Washington, DC: Society for Neuroscience, 2004. Online：http://sfn.scholarone.com/.

Yeomans, D.C., and Proudfit, H.K. (1992). Antinociception induced by microinjection of substance P into the A7 catecholamine cell group in the rats. *Neurosci.* **49,** 681-691.

Table 1. Membrane and Spike Properties of Neurons of A7 Cell Group.

	Vm (mV)	Rn* (MΩ)	Rh* (pA)	τ* (ms)	Th (ms)	SH (mV)	HW (ms)	Int (Hz)	Max (Hz)
DBH-ir (N=26)	-59±2	526±41	103±4	32±3	-32±2	110±2	3±0.1	6±0.1	16±0.4
Non DBH-ir (N=22)	-53±1	1147±152	52±4	62±7	-35±1	101±2	2.9±0.2	8±0.1	32±2.5

Vm: resting membrane potential
Rn: input resistance
Rh: rheobase
τ : membrane time constant
Th: threshold for firing
SH: spike high
HW: half width
Int: initial firing
Max: maximum firing rate
* : significant difference with $p < 0.05$

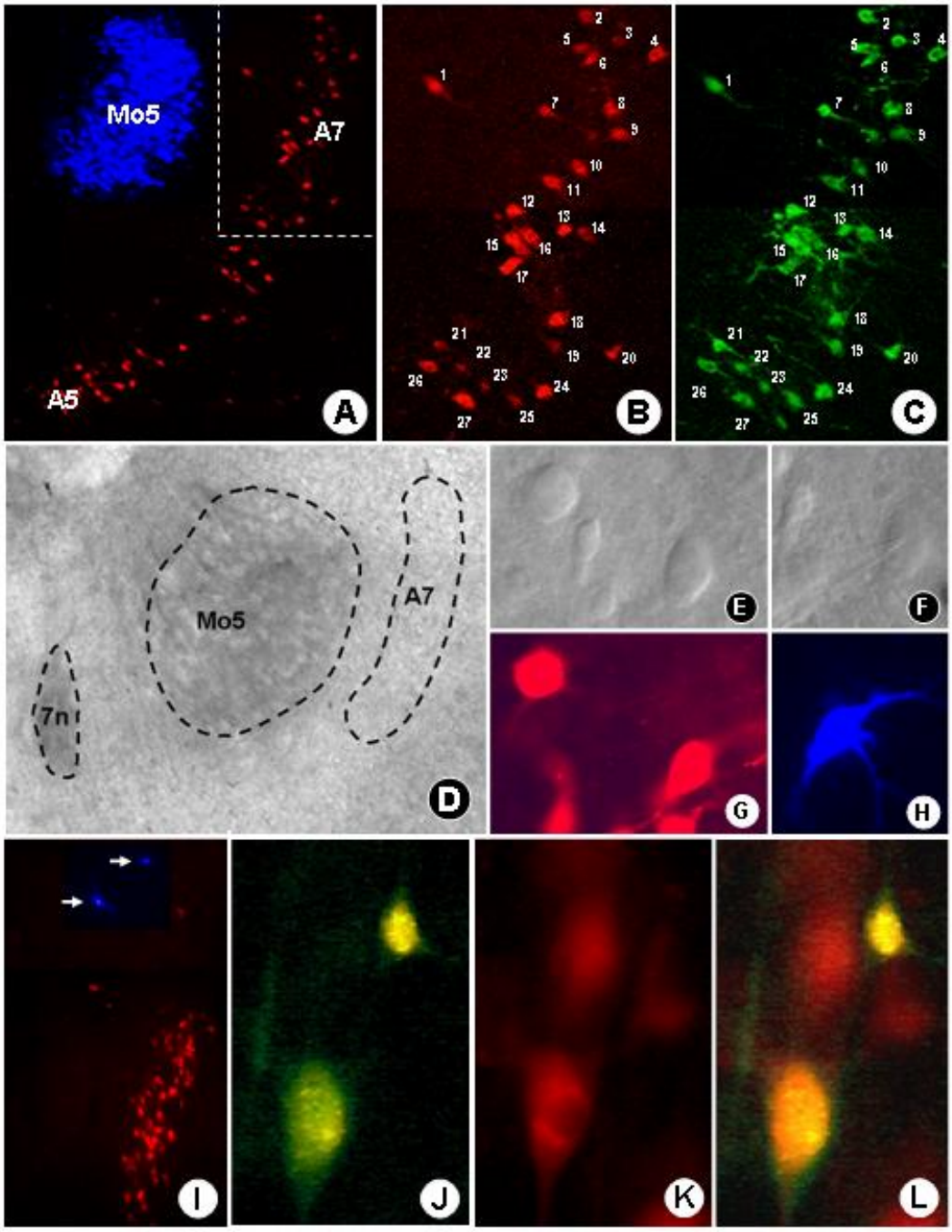
Mo5
A7
A5
A
B
C
Mo5
A7
7n
D
E
F
G
H
I
J
K
L

FIGURE 1. Identify NAergic neurons of A7 cell group in longitudinal brainstem slice.

Trigeminal motor nucleus (Mo5) was labeled by true blue (A) and NAergic neurons of A7 and A5 cell groups show both TH-ir (green) and DBH-ir (red) (A-C). Two types of neurons with different stomata diameter were identified in presume A7 area in the fresh brainstem slices using IR-DIC optics (D-F). Neurons recorded were identified by injection of biocytin (H) or Lucifer Yellow (J), and NAergic neurons were identified by immunostaining of DBH(G). Neurons recorded can be classified in to (1) non DBH-ir neurons located outside the A7 area (I), (2) non DBH-ir neurons within the A7 area (J-L), and (3) NAergic neurons in the A7 area (J-L).

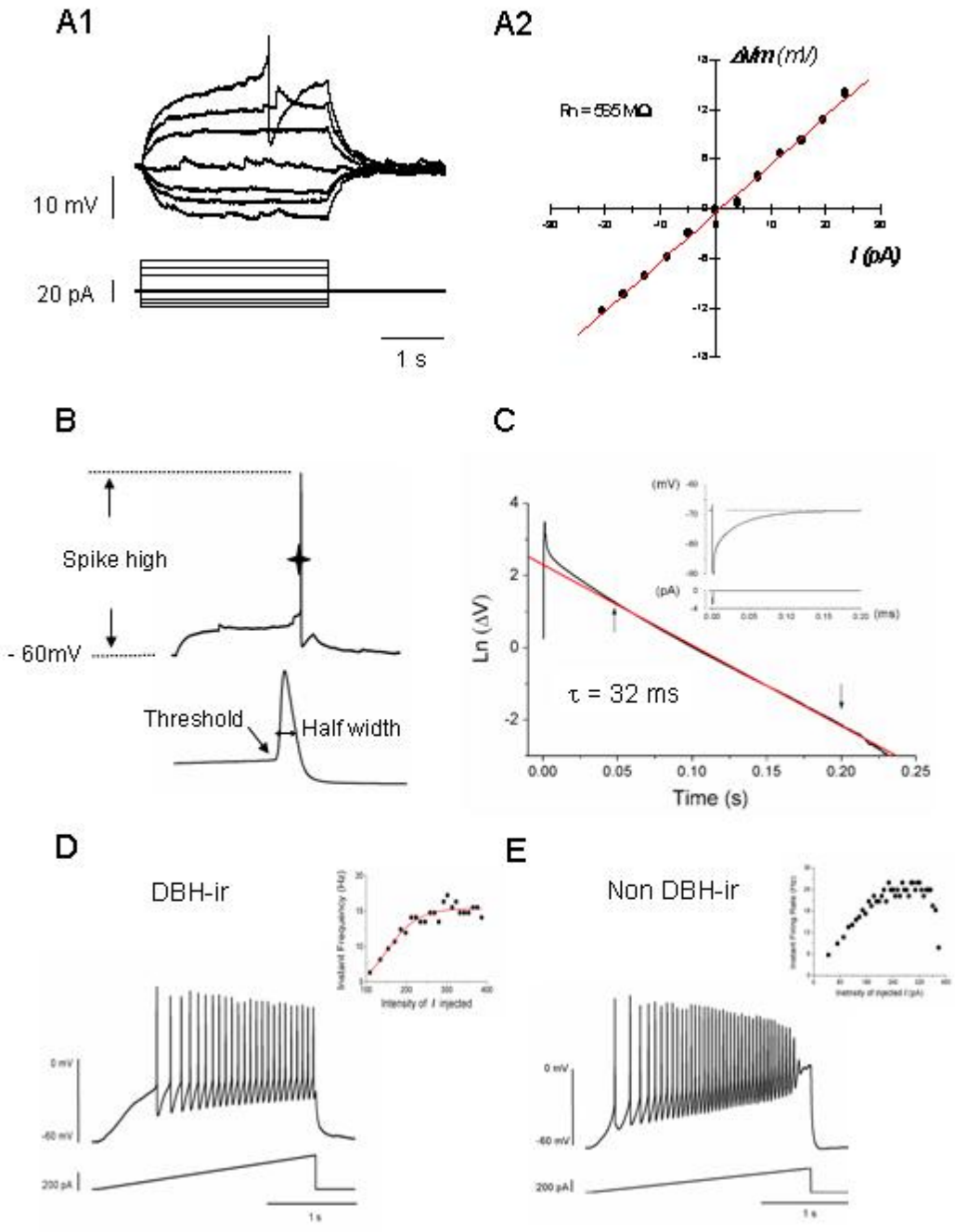
A1
10 mV
20 pA
1 s
A2
ΔVm (mV)
Rn = 555 MΩ
I (pA)
B
Spike high
- 60mV
Threshold
Half width
C
Ln (ΔV)
τ = 32 ms
Time (s)
(mV)
(pA)
(ms)
D
DBH-ir
Intensity of I injected
E
Non DBH-ir

FIGURE 2. Membrane and spike properties of recorded neurons.

Input resistance, rheobase, and membrane time constant were significant different between the DBH-ir and non DBH-ir neurons in A7 area (A, B, C; Table 1). The maximum firing rate of DBH-ir neurons is slower than the non DBH-ir neurons in response to the injection of depolarizing current ramp (D, E; Table 1).

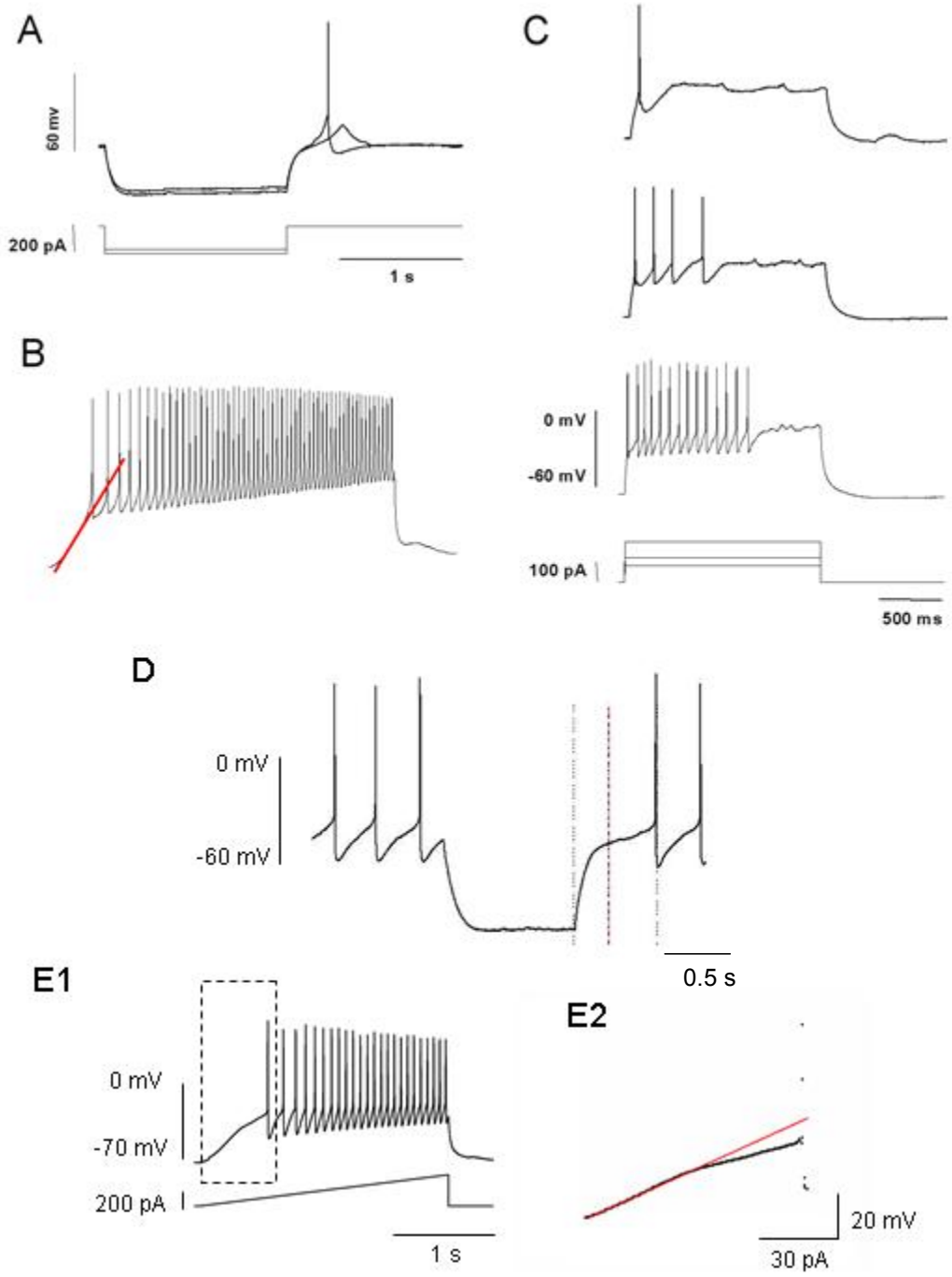
A
60 mv
200 pA
1 s
B
C
0 mV
-60 mV
100 pA
500 ms
D
0 mV
-60 mV
0.5 s
E1
0 mV
-70 mV
200 pA
1 s
E2
20 mV
30 pA

FIGURE 3. Spiking pattern of non-DBH-ir and DBH-ir neurons in A7 area.

According to firing pattern, non-DBH-ir neuron can be grouped into three categories. The first and second groups were repeatedly and regularly fired neurons with (A) or without (B) rebound action potential. The third group was neurons with significant spike adaptation (C). DBH-ir neurons showed very prominent delay in firing the first action potential upon injection of depolarizing current pulse (D). The relationship between the increasing intensity of current ramp and the increasing membrane voltage was linear (E1). Membrane voltage however showed rectification in direction of repolarization before the onset of action potential (E2).

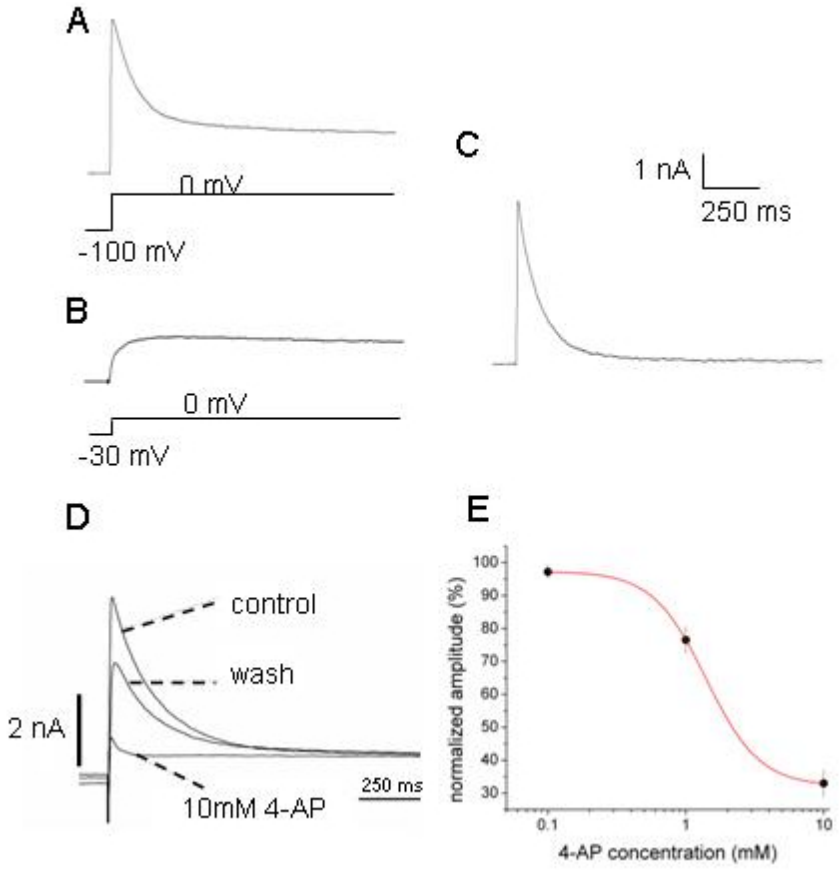
A
0 mV
-100 mV
B
0 mV
-30 mV
C
1 nA
250 ms
D
control
wash
2 nA
250 ms
10mM 4-AP
E
normalized amplitude (%)
100
90
80
70
60
50
40
30
0.1
1
10
4-AP concentration (mM)

FIGURE 4. Evocation of transient outward current and its response to 4-AP.

Transient outward current was evoked by voltage stepping from –100 to 0 mV (A). Slowly activated but sustained outward current was evoked by voltage stepping from –30 to 0 mV (B). Subtracting current evoked from –30 mV from that evoked from –100 mv yield component that, in response to voltage step, is quickly activated and completely decayed (C). The subtracted current was blocked by 4-AP, a non selective I_A blocker, with IC_{50} at 1.5 mM (D, E).

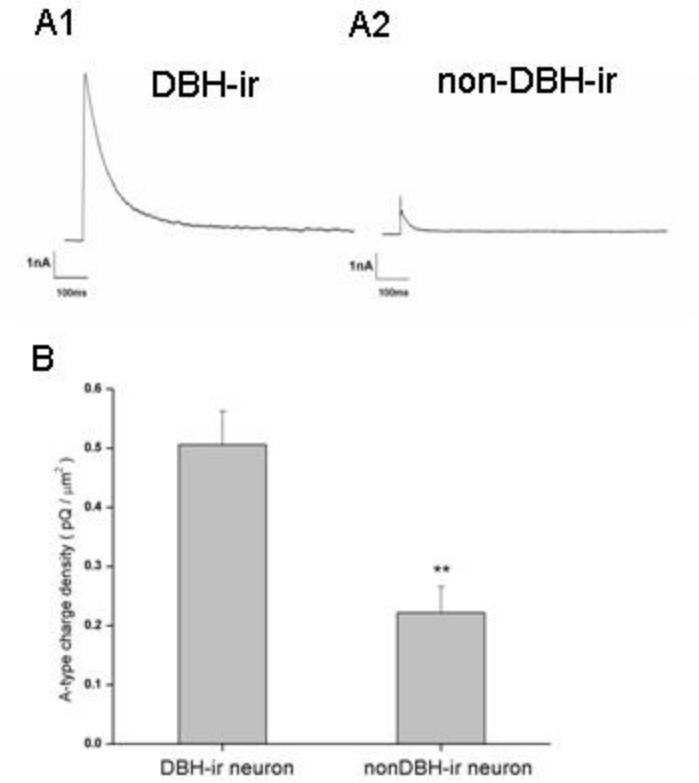
A1
A2
DBH-ir
non-DBH-ir
1nA
100ms
1nA
100ms
B
A-type charge density (pQ / μm²)
0.0
0.1
0.2
0.3
0.4
0.5
0.6
**
DBH-ir neuron
nonDBH-ir neuron

FIGURE 5. Peak amplitude and charge density of I_A in DBH-ir and non-DBH-ir neurons.

Large peak amplitude of I_A can be constantly evoked by almost all DBH-ir neurons tested (A1). Peak amplitude of I_A evoked in non DBH-ir neurons was not as large as in the DBH-ir neurons (A2). Charge density of I_A obtained from DBH-ir neurons is much higher than that obtained from that of non-DBH-ir neurons (B).

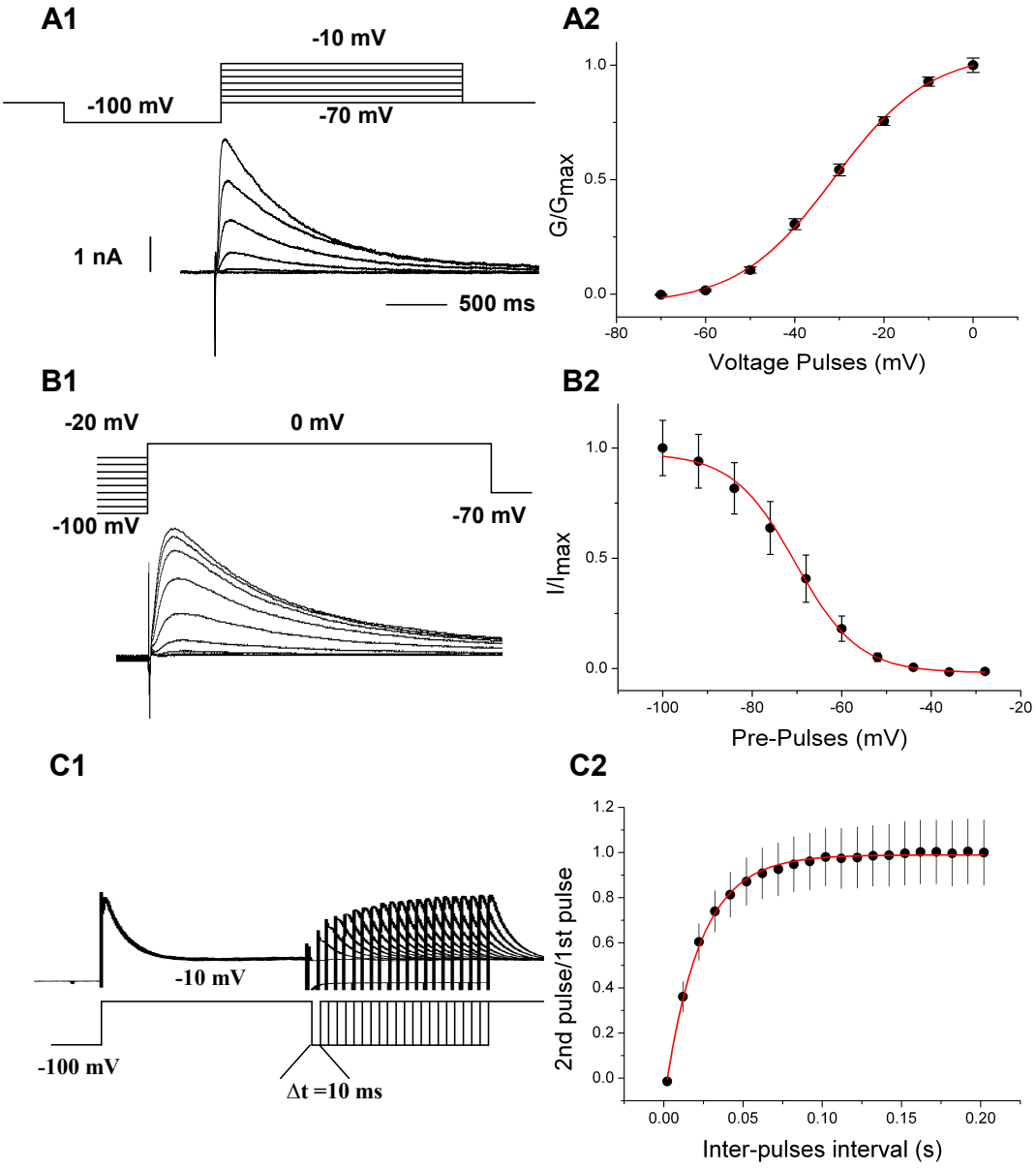
A1
-10 mV
-100 mV
-70 mV
1 nA
500 ms
A2
G/Gmax
Voltage Pulses (mV)
B1
-20 mV
0 mV
-100 mV
-70 mV
B2
I/Imax
Pre-Pulses (mV)
C1
-10 mV
-100 mV
Δt =10 ms
C2
2nd pulse/1st pulse
Inter-pulses interval (s)

FIGURE 6. The gating kinetic of I_A evoked in DBH-ir neurons.

To determine the voltage-dependent activation, voltage steps of 1 s were applied in 10 mV increments from -90 mV to a maximum of -10 mV(A1). Activation of I_A starts at –60 ~ -50 mV with half activated at about –30 mV (A2). To determine the voltage-dependent inactivation, conditioning pre-pulses ranging from -90 mV to -20 mV were applied in +10 mV increments followed by a step to 0 mV (B1). The I_A is approximately half inactivated at Vm about –70 mV (B2). To determine time-dependent recovery from inactivation, conditioning pulses were applied in 10 ms incremental duration from 10 ms to 200 ms (C1). The I_A recovers from inactivation very quickly with recovering time constant being 21.87 ms (C2).

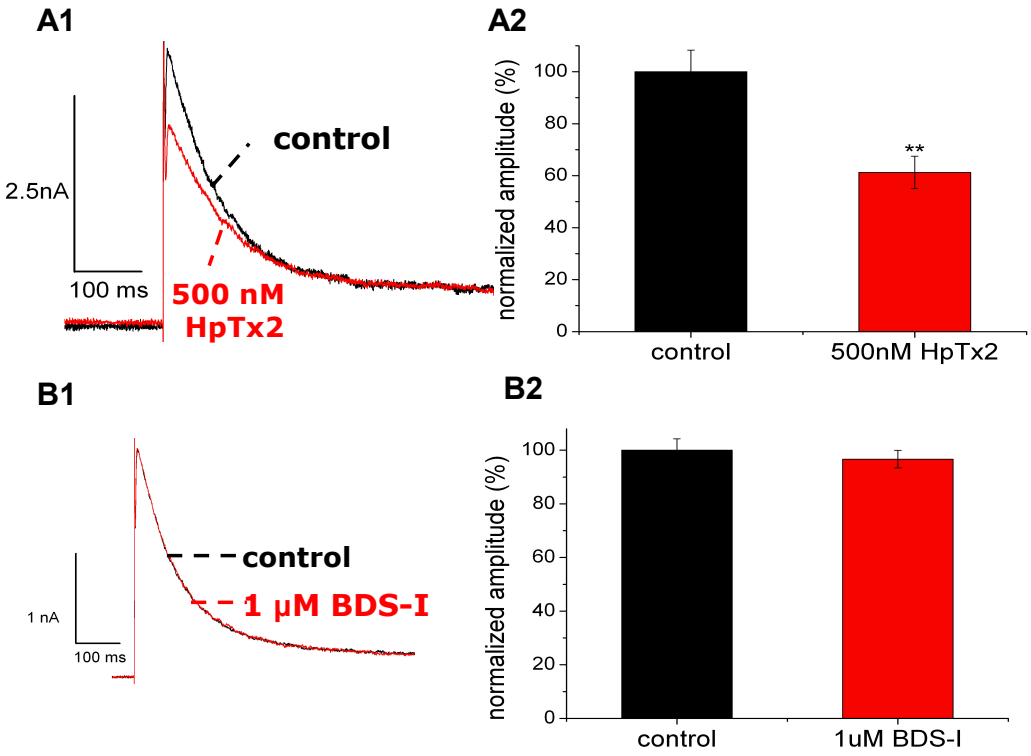
A1
2.5nA
100 ms
control
500 nM
HpTx2
A2
normalized amplitude (%)
100
80
60
40
20
0
**
control
500nM HpTx2
B1
1 nA
100 ms
control
1 μM BDS-I
B2
normalized amplitude (%)
100
80
60
40
20
0
control
1uM BDS-I

FIGURE 7. The pharmacological properties of I_A evoked in DBH-ir neurons.

The I_A evoked in DBH-ir neurons I_A is attenuated by HpTx by 38.64 % (A) (n = 4 cells tested; $p<0.01$ paired t test) in DBH-ir neurons. Application of 1 μM BDS-1 has no significant effect on I_A (96.7 % of control; n = 3; $p > 0.2$, paired t test) (B) in DBH-ir neurons.

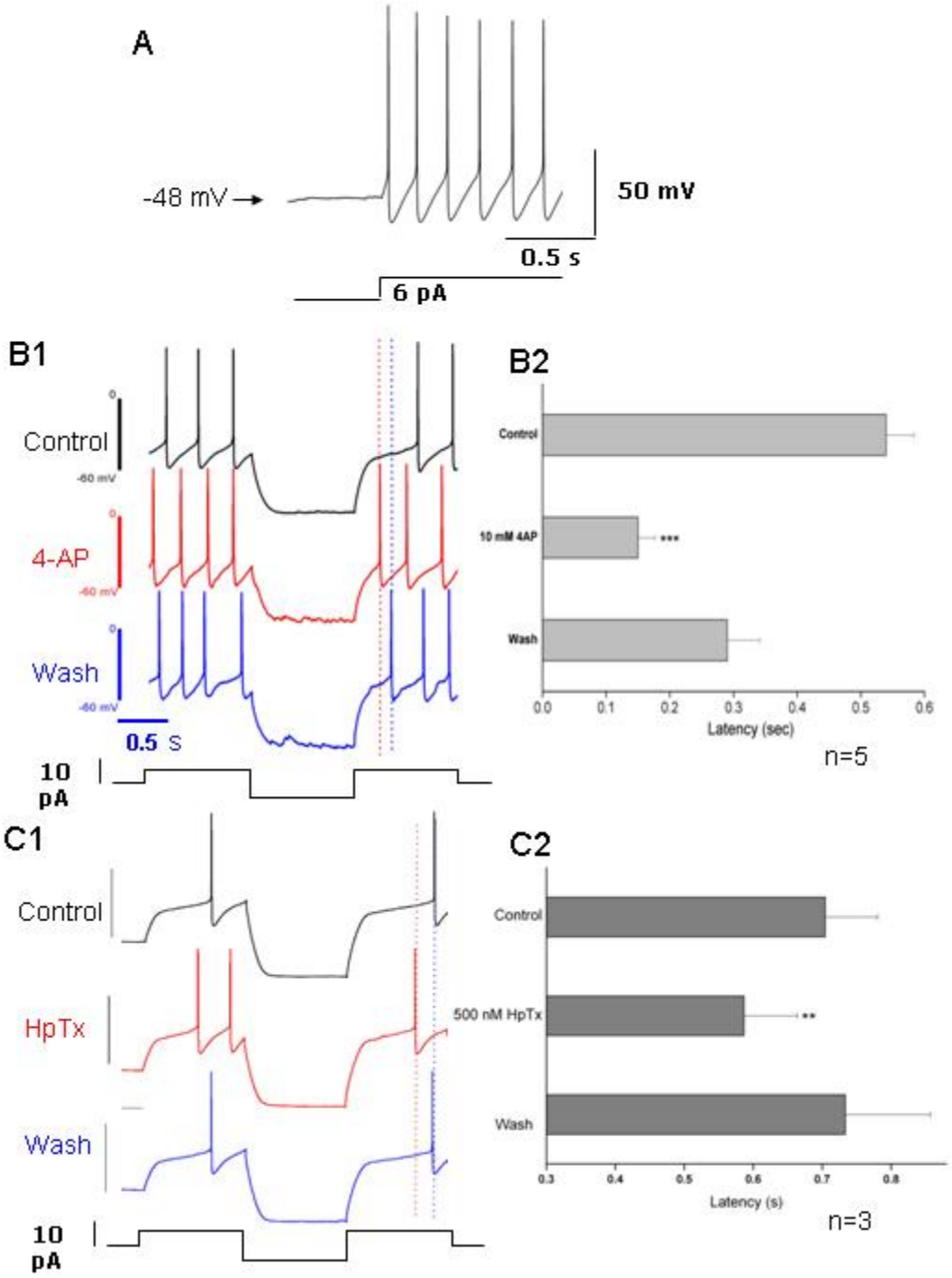
A
-48 mV
50 mV
0.5 s
6 pA
B1
Control
4-AP
Wash
0.5 s
10 pA
B2
Control
10 mM 4AP
Wash
***
0.0
0.1
0.2
0.3
0.4
0.5
0.6
Latency (sec)
n=5
C1
Control
HpTx
Wash
10 pA
C2
Control
500 nM HpTx
Wash
**
0.3
0.4
0.5
0.6
0.7
0.8
Latency (s)
n=3

FIGURE 8. Contribution of I_A to the prominent delay in firing action potential.

Delay in the initiation of action potential in response to 6 pA depolarizing current injection was not seen when the membrane potential was to about –45 mV (A). Delay in initiation of action potential was blocked by 4-AP (B) and HpTx2 (C), even when the membrane potential was hold at –80 ~ -90 mV.

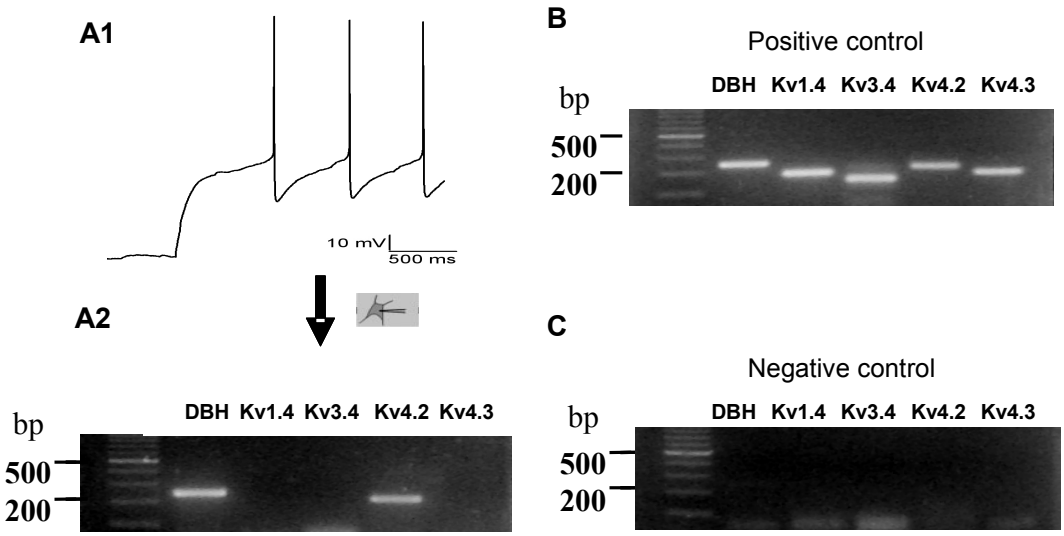
A1
10 mV
500 ms
A2
bp
500
200
DBH Kv1.4 Kv3.4 Kv4.2 Kv4.3
B
Positive control
bp
500
200
DBH Kv1.4 Kv3.4 Kv4.2 Kv4.3
C
Negative control
bp
500
200
DBH Kv1.4 Kv3.4 Kv4.2 Kv4.3

FIGURE 9. The molecular composition of A-type channels in DBH-ir neurons.

Specific primer pairs for Kv1.4, Kv3.4, Kv4.2, Kv4.3 and DBH were designed to amplify cDNA products reverstranscript from mRNA of single neuron. The cDNA of brainstem tissue were used as templates in positive control (B). The cDNA products obtained from internal solution of patch-pipette without extracting cell content were used as templates in negative control and no band was showed (C). The PCR products amplified from cDNA of the same single neuron with prominent delay in firing action potential (A1) showed the expression of both Kv4.2 and DBH (A2).